N O T I C E

THIS DOCUMENT HAS BEEN REPRODUCED FROM MICROFICHE. ALTHOUGH IT IS RECOGNIZED THAT CERTAIN PORTIONS ARE ILLEGIBLE, IT IS BEING RELEASED IN THE INTEREST OF MAKING AVAILABLE AS MUCH INFORMATION AS POSSIBLE

NASA Technical Memorandum 82678

Some Aspects of Calculating Flows About Three-Dimensional Subsonic Inlets

H. C. Kao
Lewis Research Center
Cleveland, Ohio

Prepared for the
Seventeenth Joint Propulsion Conference
cosponsored by the AIAA, SAE, and ASME
Colorado Springs, Colorado, July 27-29, 1981

NASA

Some Aspects of Calculating Flows About Three-Dimensional Subsonic Inlets

H. C. Kao
National Aeronautics and Space Administration
Lewis Research Center
Cleveland, Ohio 44135

Abstract

Based on the potential flow model, computations were carried out for various three-dimensional inlet models. Some of these calculated results are presented here in the forms of surface static pressure, flow angularity, surface flow pattern, and inlet flow field. Comparisons with experimental data are also made when available.

Introduction

Interest in developing V/STOL aircraft technology has increased considerably in recent years. As part of this endeavor, efforts are being made to contrive new designs for a propulsion system which can be operated over a wide range of flight speeds, incidence angles and throttle settings. Since an inlet is a part of this system, various configurations have been proposed. In general, these proposed inlets are three-dimensional and may even include devices such as a drooping lip, slot, slat, and blow-in doors. Because these geometries are usually considerably more complicated than the axisymmetric ones, the experimental cost in investigating them by varying different parameters is much higher. Thus, we are compelled to consider the alternatives for the preliminary screening. The fact that computational techniques have made significant improvements and can now handle some types of three-dimensional configurations prompted us to conduct an investigation of inlets by employing a computational method.

The tendency of using devices attached to the basic inlet gives rise to the need for knowing the entire or part of the flow field so that they can be judiciously placed along with local modifications if necessary. This type of information cannot be easily acquired in a wind tunnel test. It is, however, a part of the solution with most computational methods. Thus, using computational techniques provides an additional benefit.

To design an "optimum" configuation, one usually has to investigate combinations of different geometric variables and operating conditions. This requires a large number of repeated calculations. Under the present state of the art, viscous flow computations based on the Navier-Stokes equations are difficult, extremely costly, and cannot be used efficiently for parametric studies. Even obtaining numerical solutions for high subsonic or transonic flows using full potential or Euler's equations is deemed impractical for this purpose. Our approach is, therefore, to compute the incompressible potential flow. Since the governing equation is the Laplace equation, solutions can be obtained very efficiently by the surface distribution of singularities (the panel method). After the incompressible flow solution is obtained, a compressibility correction is then applied through a semi-empirical procedure to introduce compressibility effects. Although the flow field may produce embedded supersonic flow regions after correction, a subsonic incoming stream is always assumed.

Several computer programs based on the theory of distribution of singularities have been developed by various investigators and are now available. Most of these programs are mainly for external flows. The one, which we have used for internal flow calculations, is the Douglas-Neumann panel method and has several versions. Two commonly used ones for our purpose are the axisymmetric and three-dimensional subsonic inlet programs (Refs. 1 and 2). Since the latter computer program is being extended to handle more complicated three-dimensional geometries, there is a need at present to see what it can and cannot do with the present version, so that modifications may be made in the new version. The purpose of this report is, therefore, to review its capabilities and to present some results for three-dimensional inlet models. In addition, a brief discussion is included to illustrate the use of a topological rule for the presence of stagnation points.

Computer Program

In spite of the fact that panel methods are among the oldest of the various computer programs, and have perhaps reached some degree of maturity, efforts are still being made in many organizations to improve them. However, since the basic model has been fairly well established, the largest proportion of these efforts appears to be for extending the range of application, improving its accuracy and easing the user's burden. The computer programs developed in Refs. 1 and 2 fall into this category. Although the panel method in Ref. 2 can now handle three-dimensional geometry, limitations still

exist and paneling can be difficult for certain geometries. One of these is the requirement that a shroud must be constructed as a single body by a number of longitudinal lines along which the number of panels must be equal (the size of panels need not be the same). It follows that corners and other special parts of the shroud cannot be constructed separately and patched with the rest of the body. The irregular appearance of panel distribution in some of the configurations presented can be attributed to this cause.

Since the theory for the panel method, especially the Douglas-Neumann program, is well documented, only a very brief description is given here. Basically four independent solutions for four basic flow conditions are first computed: a static solution with flow into the inlet ($V_\infty = 0$) and three stream flow solutions with unit velocity vector parallel to each of the three cartesian coordinate axes of which the x-axis is the axial direction corresponding to zero angle of attack and yaw. These are the so-called fundamental solutions, which will in general be saved for the future use. From these four fundamental solutions, a combination solution is found by means of linear superposition that satisfies the flow conditions such as the angle of attack, angle of yaw, and mass flow rate specified by the user. Because of the linear superposition, the computing time for a combination solution is relatively short. Once the fundamental solutions are available for a given geometry, a large number of inlet operating conditions may be investigated with a small additional cost.

The flow quantities obtained in this manner are nominally "exact". In the situation where compressibility is important, these quantities have to be corrected for the compressibility effect. The method used here is the Lieblien-Stockman procedure (Ref. 3), which is semi-empirical. However, experience has shown that a good agreement with experiment can ordinarily be expected, especially internally, provided that the configuration is not too much different from an axisymmetric one.

The present version of the 3-D subsonic inlet program is the so-called first-order panel method. It is charcterized by approximating each (curved) panel by a plane quadrilateral on which the source strength is assumed to be constant. A control point is selected on each plane quadrilateral surface and the bondary condition of zero normal velocity component is imposed at this pont. Consequently, the source strength varies as a step function from panel to panel and the tangency condition is not assured except at control points. These first-order approximation errors are known to cancel each other to a considerable extent for convex surfaces (external flow

surfaces). However, the degree of cancellation for internal flows is much reduced. Therefore, "leakages" often occur in an inlet, especially in the vicinity in corners. The discrepancy seen between the computation and experiment of some presented cases is perhaps in part due to this problem.

Calculated Results

A. Paneling and Surface Static Pressure

Although a considerable effort was made to assess the accuracy of the 3-D subsonic inlet code by treating (pretending) axisymmetric inlets as three-dimensional ones, the first real attempt of using this code was for the scoop and scarf inlet models tested in the NASA-Lewis' wind tunnel. The reason for selecting this class of configurations is two-fold. First, it has shown sufficient advantages over the axisymmetric baseline geometry to warrant a further study (Fig. 1). Second, both the geometry and the flow distribution are sufficiently three-dimensional to render the "strip" or other equivalent methods inapplicable, and at the same time it is not a complex geometry.

Geometry: Both a scoop and scarf inlet are characterized by having a longer lower lip than the upper lip. The difference between them is that a scoop inlet has an abrupt transition from the long lower lip to the short upper lip (Fig. 4) and a scarf inlet has a straight-line smooth transition (Fig. 5). The lengths of the lower lip and upper lip for both inlet models are, however, the same. When the added length to form the scoop or scarf inlet becomes zero, it is reduced to the baseline geometry, which is axisymmetric (Fig. 3). Thus, apart from added lengths on the lower lips of the scarf and scoop inlets, all three inlet models have the identical geometry. Their dimensions and design parameters can be found in Ref. 5.

Observed Properties: It appears that the effect of an extended lower lip in a scoop or scarf inlet is to provide a "barrier", which obstructs the path for an easy access from the lower portion. Thus, the capture streamtubes are forced to bend upward, as shown schematically in Fig. 1, to create an apparent effect of a negative angle of attack. As a result, it gives a higher flow separation bound at positive angles of attack as amply confirmed by the measurements made in Refs. 4 and 5. Although both the scoop and scarf inlet models have exhibited this performance advantage, the former tends to have larger total pressure losses at the sides than the latter. In order to prevent this adverse effect, the scarf inlet model with a smooth transition was designed and subsequently tested. In effect, it supersedes the scoop inlet.

The cause of the total pressure losses at the sides of a scoop inlet is usually attributed to the possible presence of two vortices induced by the abrupt transition of the profile (Ref. 4). Here we make an attempt to argue that the flow properties based on the potential flow calculation alone give sufficient evidence in favor of the scarf inlet model. This is considered to be of some significance, since only the potential flow calculations and empirical criteria will be used at present for the preliminary screening, which do not take vortices into account.

It is desirable to choose a representative set of flow conditions for all three models, so that one can focus his attention and make comparisons. These conditions are indicated in Figs. 3-7, and are the same as those used by Abott in presenting his test data (Ref. 5). In Figure 2, we notice that the surface static pressure at the highlight of the scoop and scarf inlet varies considerably from the bottom to top with a zero freestream velocity. This is an indication of the flow three-dimensionality, since this surface pressure distribution is nearly uniform for the baseline axisymmetric inlet.

Prior to computation, we have to represent the geometry in the form of panels. Portions of these panels are plotted in Figs. 3-5. Not shown are the centerbody and the artificial cylinder added behind the fan face. The purpose of adding an artificial cylinder, which is often several inlet diameters long, is to reduce the influence of the exit on the fan face. The total number of panels, including the shroud, centerbody and the artificial cylinder, is approximately 700 for these inlet models.

After paneling is completed, we can then proceed with computation. The longitudinal surface static pressure distributions for these inlet models are shown in Figs. 3-5 along with measurements made in Refs. 4 and 5. In addition, flow angularities at the throat station and at a station slightly upstream of the fan face are plotted in Figs. 6 and 7. These are the angles formed between the axial (normal to the cross-sectional surface) and z velocity components, where z is the axis situated on the plane of symmetry with the positive direction pointing upward. Thus, a positive angle in these figures implies that the local velocity vector has an upward inclination.

From Figs. 3-5, we notice the following: The lower lip of the baseline geometry is highly loaded (low static pressure), and the adverse pressure gradient is the severest among all the stations shown in these figures. As the lower lip extends forward to form a scoop or a scarf inlet, the loading is redistributed, which results in reducing the loading for the

lower lip and increasing it at the upper lip. Consequently, a substantial total pressure loss, if it occurs, will begin at the upper portion of the inlet. A fluid particle undergoes a more rapid turning in the upper part than in the lower one. This inverse distribution of loading for a scarf inlet model changes monotonically from the lower value at the lower lip to the higher value at the upper lip. However, it is different with the scoop inlet model. The upper lip is not the highest loaded one; instead it occurs in the middle of each of the two upper quadrants. Referring to Fig. 4, we notice that the graphs for the static pressures of the scoop inlet are arranged in the clockwise direction for $\theta = 0^0$, 90^0, 135^0 and 180^0 with θ denoting the circumferential position and the windward station at the bottom of the figure being at $\theta = 0$. The third station with $\theta = 135^0$ refers to the middle of the upper quadrant, where the static pressure in the lip region is lower than those for its two neighboring stations. Hence, the flow has the tendency to converge circumferentially to the middle that may promote the formation of the vortices.

Our point of view that the scarf inlet model shows more favorable features than the remaining two is further strengthened after examining the flow angularities in Figs. 6 and 7. The flow angularity gradient for the baseline inlet appears to be fairly concentrated in the upper portion of the throat station (Fig. 6), but it flattens out in the diffuser and becomes somewhat uniform near the fan face (Fig. 7). (The throat station here refers to the throat station based on the upper most profile.) On the contrary, the flow angularity gradient for the scoop inlet is moderately uniform at the throat station, but it steepens in the diffuser and becomes more concentrated near the fan face, as is evident in the two regions at the sides of the scoop inlet in Fig. 7. Although the density of lines do not appear to be large due to the fact that the increment of contour lines is 2^0 instead of 1^0, the flow angles change from -4^0 to 2^0 in a short distance. As for the scarf inlet, it is seen that the flow angularity gradient is the smallest among three models at both the throat station and near the fan face.

In conclusion, it appears that some of the salient features for these models are predictable through the inviscid flow calculations. Even the abrupt change in the inlet profile may be detected through examining the local flow properties.

B. Surface Flow Pattern

Detailed flow field surveys are seldom made, when inlet models are tested in wind tunnels especially outside of the shroud and on the surface. The recent tendency of using devices attached

to the basic inlet to cope with high angle-of-attack problems may demand some understanding of the flow property surrounding the particular device before and after its installation. Therefore, it is useful to conduct such a study based on numerical computation. We will discuss the surface flow pattern here and defer to the next section for a discussion of the flow field outside the shroud.

In order to determine the capture streamtube, one usually initiates either from an upstream station proceeding forward or from the surface proceeding backward. The former approach may require many iterations; the latter may avoid iteration but requires knowing the surface velocity distribution and devising a procedure to initiate velocity vector tracking. Thus, knowing the surface flow pattern especially near the dividing streamlines may provide some useful information for determining capture streamtubes.

After the existence of stagnation points in the flow field was found by using the axisymmetric inlet computer program in Ref. 6, Stockman initiated an inquiry about the surface stagnation points (private communication). Although his effort was not continued, it gave an impetus for the present work.

Based on the same computer output used for Figs. 3-7, we plot the surface flow pattern in the forward sections of the baseline, scarf and an axisymmetric shroud in Figs. 8 and 9. In these figures, we notice that the rear sections are excluded, some panels are removed, and a cut-off length for the velocity vectors is imposed. By doing this, though the pictures are less realistic, they are less cluttered and easier to read. Moreover, no hidden line removal procedure is used in plotting velocity vectors. Consequently, those vectors on the lower part of the scarf inlet lip, which may appear to be inside, are actually on the exterior surface. In Fig. 8, the first and last velocity stations are on th left-hand side of the plane of symmetry. Thus, the plane of symmetry lies between the first and second velocity station and between the last and next to the last station. In Fig. 9, the first and last station are also on the left-hand side of the symmetric plane, but the plane of symmetry passes through the second velocity and next to the last velocity station.

From these figures, it is possible to perceive the approximate location of the highlight and notice that there are two groups of velocity, some of which are pointed forward and the rest pointed backward. We believe that the line between them, regarded as the dividing line here, is the intersection curve of the capture streamtube.

The general appearance of the velocity vectors in these figures, except those near the plane of symmetry, has the tendency of upward motion. This is due to the fact that inlets are under positive angles of attack. Since these inlets have a plane of symmetry, the upward motion, i.e., the circumferential components, must reduce the zero at the plane of symmetry as is most evident in the upper part of Fig. 9. (it is not so evident in Fig. 8 because the plane of symmetry does not contain velocity stations, but the circumferential components reverse their direction across the plane of symmetry that implies zero components.) Consequently, the velocity vectors must all be longitudinal there. However, since the capture streamtube cuts across the plane of symmetry, these longitudinal velocity vectors direct either forward or backward and there is at least one point where the velocity is zero, that is the stagnation point.

There are actually two stagnation points in the forward section of a shroud of which one is on the windward side and the other one the leeward side. The one on the windward side is a node point where the velocities radiates from the stagnation point, whereas the one on the leeward side is a saddle point where the fluid converges from the two sides, meets at the stagnation point and splits into the forward and backward direction. This is in contrast with a closed body such as a sphere which often has only two node-type stagnation points. The forward one has velocity vectors all radiating from it and the backward one has velocity vectors all converging to it. The classification of a stagnation point into a node and saddle point is of some importance for the later discussion. It is explained in books on differential equations (see, for example, Ref. 7)

Both stagnation points perceived in Fig. 8 are on the exterior surface. The position of the windward stagnation point appears to be fairly strongly dependent upon the angle of attack. However, the leeward stagnation point can be displaced to the interior surface simply by reducing the mass flow rate. For example, if the mass flow rate is reduced to the half of the representative value and the other conditions remain unchanged, the leeward stagnation point will be located in the interior surface of the baseline shroud. The flow pattern is very similar to the one indicated in Fig. 9, which is taken directly from an existing example.

Furthermore, it appears that the position of the stagnation points is not strongly affected by reducing the freestream velocity. For example, reducing the freestream velocity to the half of the representative value and holding the other conditions fixed do not appear to change greatly their positions, yet the area of the capture streamtube at the far upstream is doubled.

The above discussion is essentially based on the results of numerical computation. We may, however, enhance our understanding by introducing topological rules. Application of these rules has become more common recently (Refs. 8 and 9), because it helps to interpret complex flow patterns. Usually there are special points existing on the surface of a flow pattern such as the stagnation, separation, reattachment and vortex points. These are regarded as singular points in topology and their existence is governed by topological rules (Ref. 10).

In topology a body may be transformed into another body by elastic deformations. Two bodies of vastly different appearance may actually belong to the same topological equivalence class. For instance, a shroud such as the ones in Fig. 1 is topologically equivalent to a one-fold torus, a donut-like configuration. Thus, their Euler characteristic, which is invariant for bodies of the same class, is the same. It tells us that on the surface of a shroud there must be an equal number of saddle-like and non-like stagnation points. including the possibility of funding another pair of stagnation points in the exit section (a node-like and a saddle-like stagnation point are considered to be a pair). Notice that we tacitly assume that stagnation points are the only type of singularities found on the surface, since others are caused by the viscous effect.

If a shroud is completely three-dimensional with no plane of symmetry and is at an angle of attack, stagnation points may be anywhere on the surface. However, they must exist in pairs, since a completely three-dimensional shroud is still equivalent to a one-fold torus.

In case there is a blow-in door on a shroud, it is no longer equivalent to a one-fold torus but to a two-fold torus (a donut with two holes) and the topological properties are different. In this case, the total number of saddle-like stagnation points on the surface will be two more than that of the node-like ones.

Finally we mention parenthetically that we actually performed a numerical computation to illustrate the property of the Euler characteristic. In order to form a complex geometry, we used a sufficiently thick "pylon" to join the shroud and a ellipsoidal centerbody. In this manner, it is topologically equivalent to a one-fold torus. From the computed results, we found many stagnation points but they were all in pairs.

C. Inlet Flow Field

We have presented surface flow patterns to show the stagnation points and the dividing streamlines. However, it also appears

that stagnation points may exist in the flow field under certain conditions. A sample case is given in Fig. 10 and it is on the leeward side of the plane of symmetry. A similar pattern also exists on the windward side of the plane of symmetryexcept that its position is further downstream. In this figure we notice that there is a sizable zone of small velocity surrounding the stagnation point. We further notice that the outline of the capture streamtube is discernable.

The presence of these zones of small velocity is not very sensitive to the change of the angle of attack. In fact, their existence is still detectable with the angle of attack reduced from the present value of 53^{0} to 43^{0}. They, will however, disappear fairly quickly in the regions away from the plane of symmetry. This is due to the fact that the circumferential velocity is not zero there.

Although finding stagnation points in the flow field is somewhat unexpected, their existence may be argued physically. The suction in the diffuser will in general induce some backward motion in the field, if there is no incoming velocity. This backward motion may be sufficiently large to cancel the forward motion of the incoming flow in certain areas of the flow field, as these two are combined. When this happens, stagnation points in the flow field appear. This is perhaps also the reason that they are found only when the ratio between the control station and freestream velocity is very large.

Concluding Remarks

In order to demonstate that useful information for initial screenings may be obtained from potential flow calculations, we focused our attention on a class of inlets, which are the baseline, scoop and scarf inlet models, and made an assessment on their relative merit. The computation indicates that the extension of the lower lip can reduce the adverse pressure gradient and increase the flow separation bound. In addition, surface flow patterns, the nature of stagnation points and the inlet flow field are presented. Some of these features may be helpful in modifying a design.

References

1. Stockman, N. O. and C. A. Farrell Jr.: "Improved Computer Program for Calculating Potential Flow in Propulsion System Inlets," NASA TM-73728, 1977.

2. Hess, J. L., D. P. Mack and N. O. Stockman: "An Efficient User-Oriented Method for Calculating Compressible Flow in and about Three-Dimensional Inlets," Douglas Aircraft Co., Inc., Long Beach, CA., MDC-J7733, Apr. 1979. (NASA CR-159578)

3. Lieblein, S. and N. O. Stockman: "Compressibility Correction for Internal Flow Solutions," Journal of Aircraft, Vol. 9, No. 4, Apr. 1972, pp. 312-313.

4. Abbot, J. M.: Aeroacoustic Performance of a Scoop Inlet. NASA TM-73725, 1977.

5. Abbott, J. M.: Aerodynamic Performance of Scarf Inlets. NASA TM-79055, 1979.

6. Stockman, N. O.: Recent Applications of Theoretical Analysis to V/STOL Inlet Design. NASA TM-79211, 1979.

7. Kaplan, W.: Ordinary Differential Equations. Addison-Wesley Publishing Co., Inc., Reading, Mass. 1958.

8. Hunt, J.C.R., C. J. Abell, J. A. Peterka and H. Woo: "Kinematical Studies of the Flows Around Free or Surface-Mounted Obstables; Applying Topology to Flow Visualization", Journal of Fluid Mechanics, Vol. 86, Part 1, May 1978, pp. 179-200.

9. Tobak, M. and D. J. Peake: "Topology of Two-Dimensional and Three-Dimensional Separated Flows," AIAA Paper 79-1480, July 1979.

10. Graham Flegg, H.: From Geometry to Topology, Crane, Russak & Co., Inc., New York, 1974.

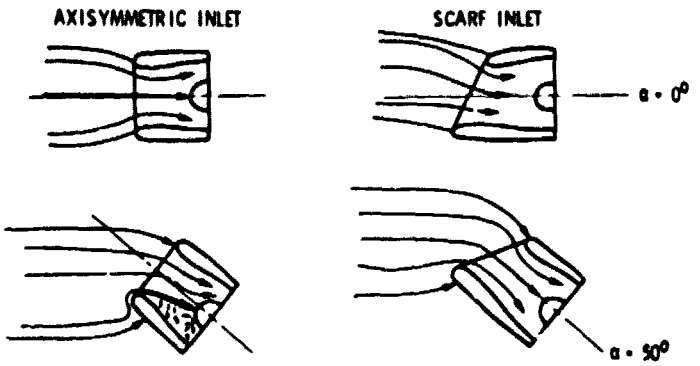

Figure 1. - Schematic depiction of inlet flow fields (ref. 5).

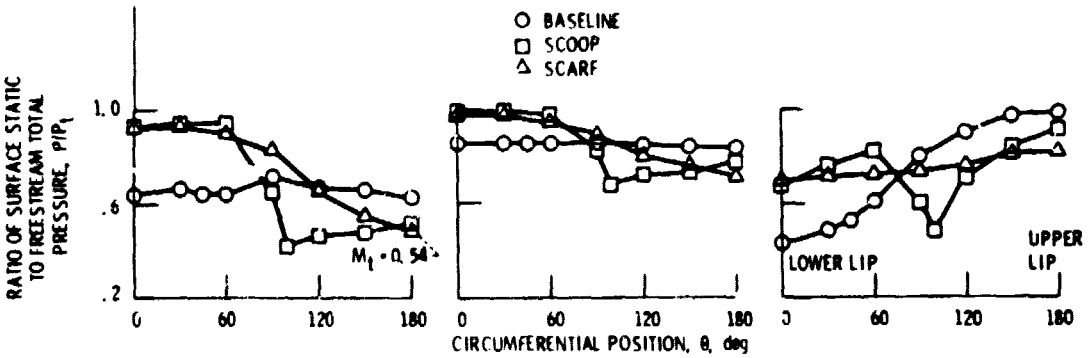

(a) FREESTREAM VELOCITY, V_∞, 0.

(b) FREESTREAM VELOCITY, V_∞, 41 METERS PER SECOND; ANGLE OF ATTACK, α, 0°.

(c) FREESTREAM VELOCITY, V_∞, 41 METERS PER SECOND; ANGLE OF ATTACK, α, 50°.

Figure 2. - Circumferential variation of measured surface static pressure at highlight. Inlet throat Mach number, M_t = 0.63 except as indicated (ref. 5).

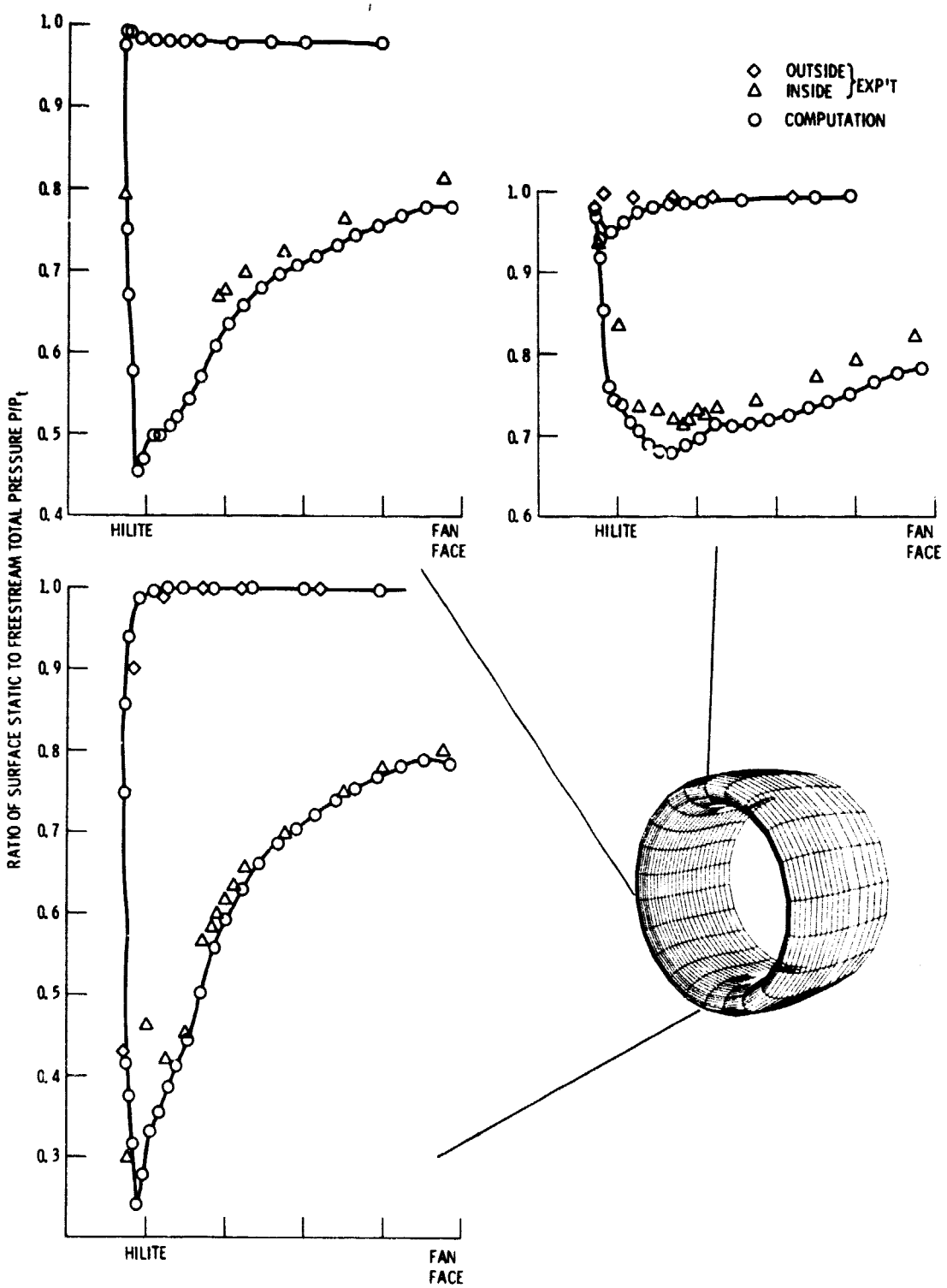

Figure 3. - Paneling and axial surface static pressure for a baseline inlet model $\alpha = 50^0$, $V_\infty = 41$ m/sec, $M_t = 0.63$ (throat Mach number).

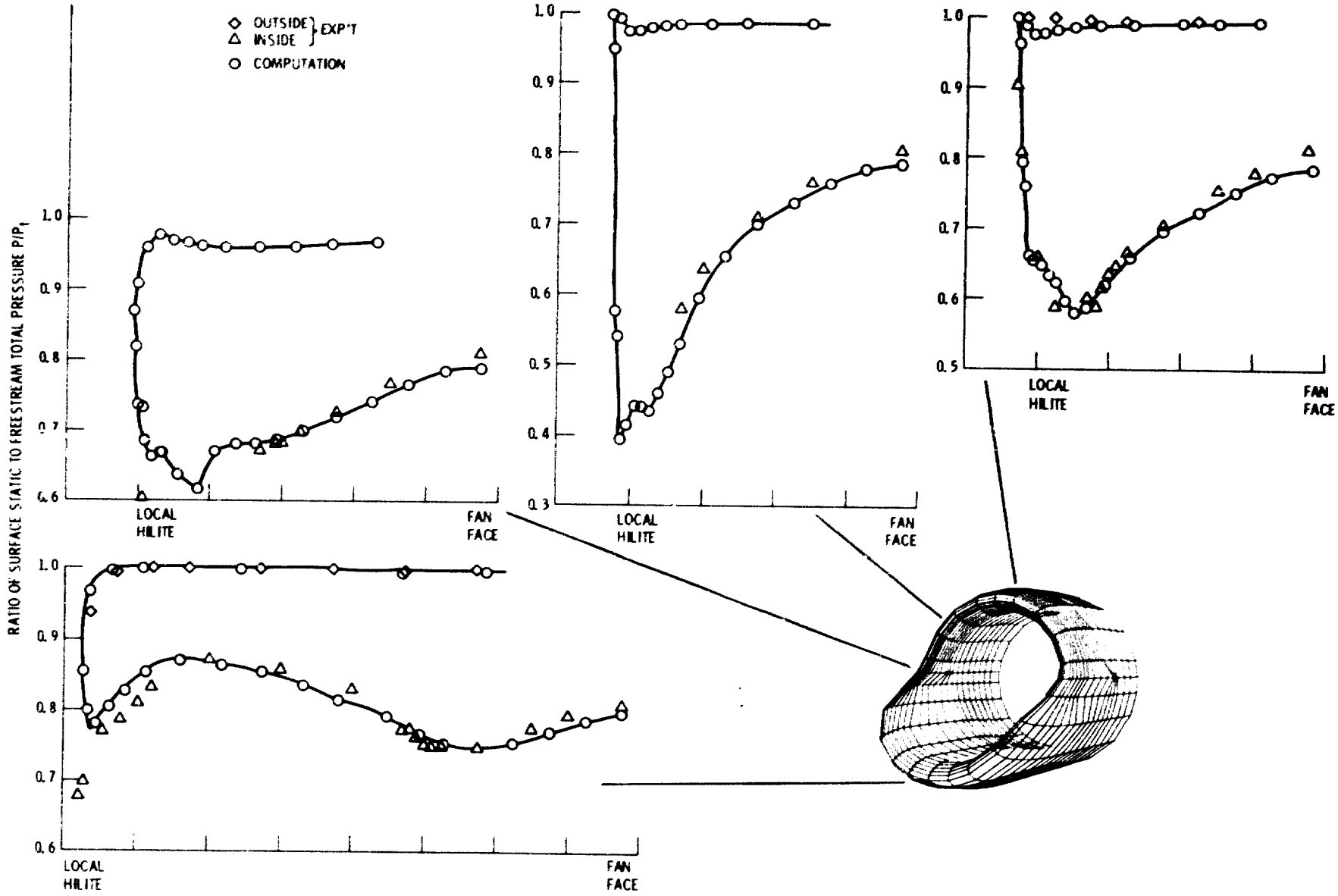

Figure 4. - Paneling and axial surface static pressure for a scoop inlet model $\alpha = 50^0$, $V_\infty = 41$ m/sec, $M_t = 0.63$ (throat Mach number).

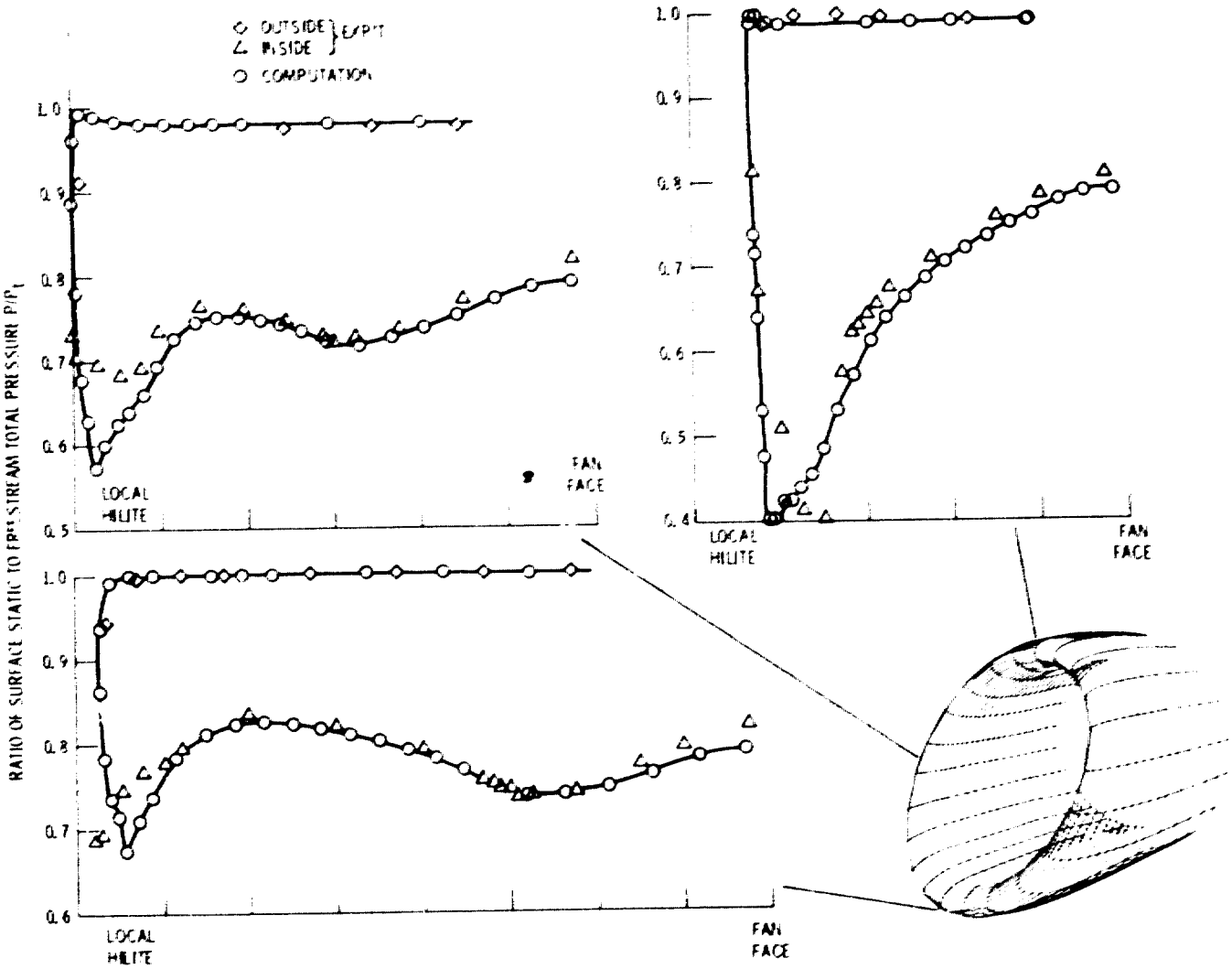

Figure 5. - Paneling and axial surface static pressure for a scarf inlet model. $\alpha = 50^0$, $V_\infty = 41$ m/sec, $M_t = 0.63$ (throat Mach number).

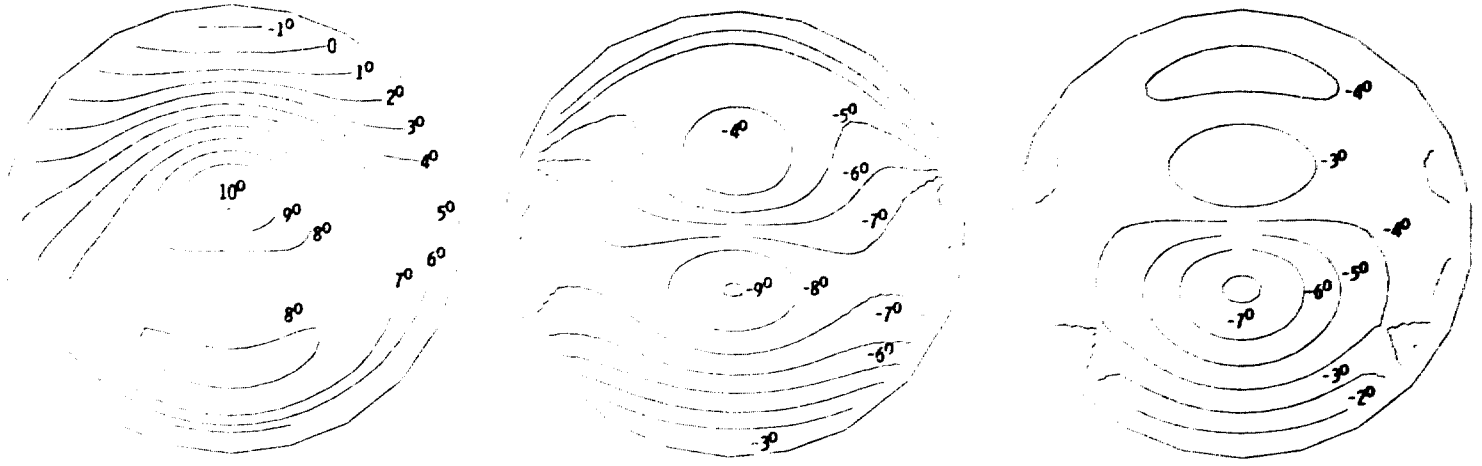

BASELINE INLET MODEL SCOOP INLET MODEL SCARF INLET MODEL

Figure 6. - Flow angularity of three inlet models at throat station in degrees between normal and z componets of local velocity $\alpha = 50^0$, $V_\infty = 41$ m/sec, $M_t = 0.63$.

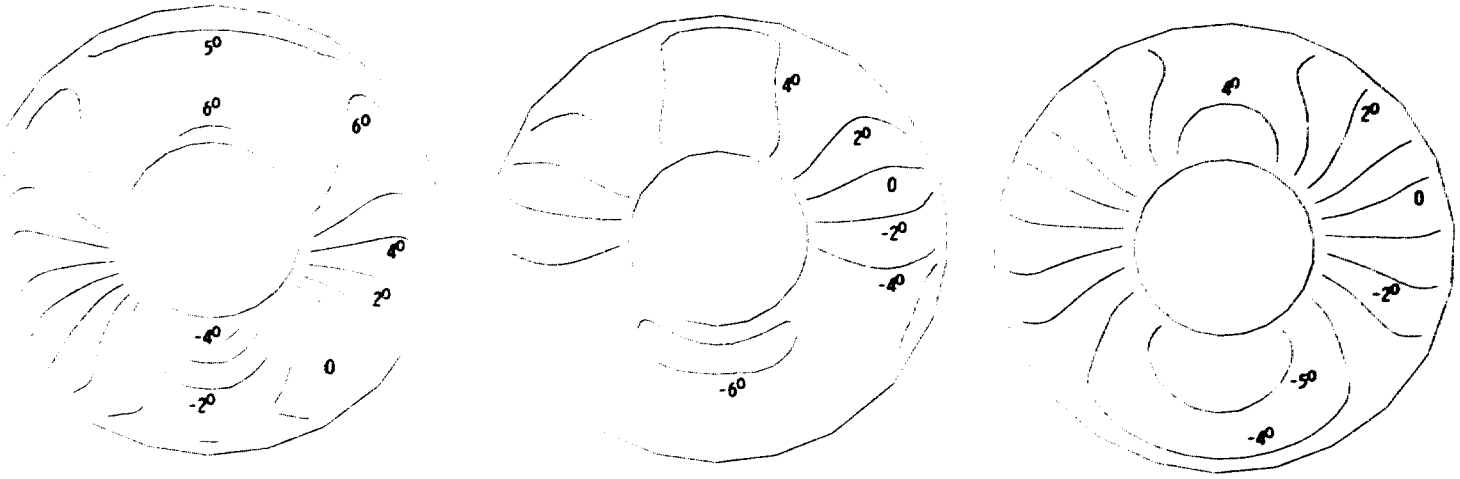

BASELINE INLET MODEL SCOOP INLET MODEL SCARF INLET MODEL

Figure 7. - Flow angularity of three inlet models near fan face indegrees between normal and z components of local velocity $\alpha = 50^0$, $V_\infty = 41$ m/sec, $M_t = 0.63$.

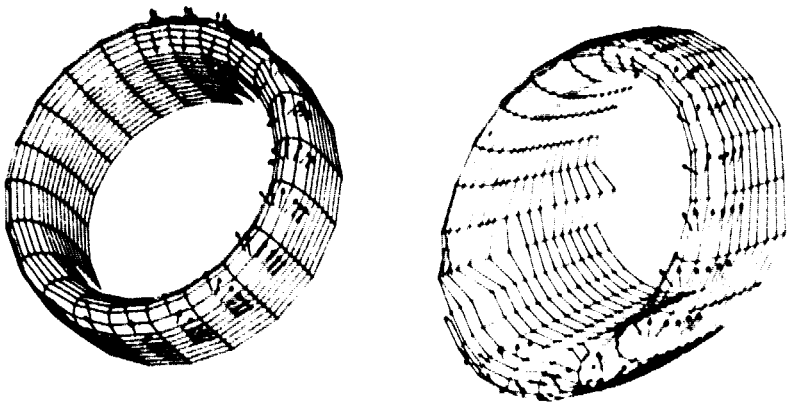

Figure 8. - Surface velocity distribution on a baseline and scarf inlet model $\alpha = 50^{0}$, $V_{\infty} = 41$ m/sec, $M_{\infty} = 0.63$. (A predetermined maximum length is used to shorten velocity vectors.)

Figure 9. - Surface velocity distribution on an axisymmetric inlet model $\alpha = 40^{0}$, incompressible flow, $V_{T}/V_{\infty} = 1.5$ (throat to freestream velocity ratio). (A predetermined maximum length is used to shorten velocity vectors.)

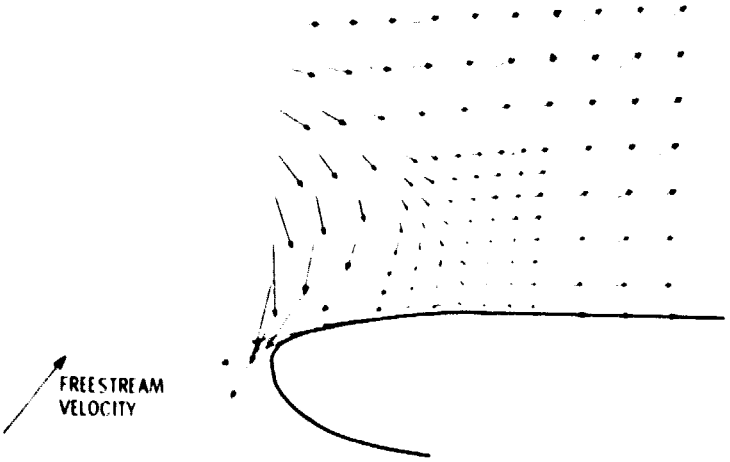

Figure 10. - Inlet flow field at leeward plane of an axisymmetric inlet model $\alpha = 53^{0}$, incompressible flow, $V_{T}/V_{\infty} = 10$ (throat to freestream velocity ratio). (A predetermined maximum length is used to shorten velocity vectors.)